Entangled Terahertz Photon Emission from Topological Insulator Quantum Dots

Li-kun Shi,[1] Kai Chang,[2] and Chang-Pu Sun[1]

[1]*Beijing Computational Science Research Center, Beijing 100193, China*

[2]*SKLSM, Institute of Semiconductors, Chinese Academy of Sciences, P.O. Box 912, Beijing 100083, China*

We propose an experimentally feasible scheme for generating entangled terahertz photon pairs in topological insulator quantum dots (TIQDs). We demonstrate theoretically that in generic TIQDs: 1) the fine structure splitting, which is the obstacle to produce entangled photons in conventional semiconductor quantum dots, is inherently absent for one-dimensional massless excitons due to the time-reversal symmetry; 2) the selection rules obey winding number conservation instead of the conventional angular momentum conservation between edge states with a linear dispersion. With these two advantages, the entanglement of the emitted photons during the cascade in our scheme is robust against unavoidable disorders and irregular shapes of the TIQDs.

PACS numbers: 03.67.Bg, 71.70.Gm, 73.21.La, 78.67.-n

arXiv:1601.04722v3 [cond-mat.mes-hall] 1 Feb 2016

Introduction.— Entanglement is the heart of quantum physics and quantum information technology[1–3]. Semiconductor quantum dots (QDs), named as artificial atoms, are one of the most promising sources for quantum light, e.g., single photon and entangled photon pair [4–21], because, comparing with real atoms and other sources, QDs possess an unique advantage of being compatible with well-developed semiconductor integration[17, 19] as well as on-demand and non-probabilistic feature[5, 6, 18] of biexciton cascade emission in QDs. The fine structure splitting (FSS), the energy difference existing between two bright exciton states in QDs with unavoidable irregular shapes, strongly spoils the entanglement of the emitted photons[8]. To overcome the FSS brought by breaking of rotational symmetry, various methods such as sophisticated QD growth control[9, 10, 14, 17, 19], external electric[13], magnetic[8], and strain fields[15, 16, 20, 21], have been used to manipulate and/or suppress the FSS of excitons in semiconductor QDs. However, for practical devices with large numbers of QDs differ from dot to dot, it is a great challenge to scale all the QDs at the same time. Therefore, QDs having no FSS intrinsically, regardless of random alloy distributions and other uncontrollable effects, are essential to realize integrated entangled photon emitters.

In this Letter, we show emitters composed of topological insulator quantum dots (TIQDs) can produce terahertz photon pairs with robust entanglement. We first present the theory in detail with a HgTe QD to illustrate our main ideas and notations. Then we prove by the time-reversal symmetry (TRS) and winding number conservation, one-dimensional (1D) massless excitons in generic TIQDs with random disorders and morphology fluctuations are free from FSS, and the entanglement of the produced photon pairs from the cascade process is robust.

Topological insulator quantum dots.—We consider a superconductor-TIQD hybrid system[22] as an example: a TIQD is fabricated in a CdTe/HgTe/CdTe heterostructure by etching technique, and it is weakly coupled to superconducting (SC) leads on two sides at p- or n-type regime, respectively [see Fig. 1 (a)]. The low-energy electron states in the *isolated* HgTe QD are described by a four-band effective Hamiltonian in the basis $|e,\uparrow\rangle$, $|hh,\uparrow\rangle$, $|e,\downarrow\rangle$, and $|hh,\downarrow\rangle$[23, 24]:

$$H_{4\times4}=\begin{bmatrix} H_{\uparrow}(\hat{\mathbf{k}}) & 0 \\ 0 & H_{\downarrow}(\hat{\mathbf{k}}) \end{bmatrix}+V(r)\,, \tag{1}$$

where $\hat{\mathbf{k}}=(\hat{k}_x,\hat{k}_y)$ is the in-plane wavevector, $H_{\uparrow}(\hat{\mathbf{k}})=H^{*}_{\downarrow}(-\hat{\mathbf{k}})=\epsilon(\hat{k})I_{2\times2}+d_i(\hat{\mathbf{k}})\sigma^i$, and σ^i $(i=1,2,3)$ are the Pauli matrices; $\epsilon(\hat{k})=C-D\hat{k}^2$, $d_{1,2}(\hat{\mathbf{k}})=A\hat{k}_{x,y}$, and $d_3(\hat{k})=M-B\hat{k}^2$. The parameters A, B, C, D, and M depend on the thickness of the HgTe layer. M is used to describe the band insulator with a positive gap ($M>0$) and non-trivial topological insulator with a negative gap ($M<0$). The hard-wall confining potential $V(r)$ is employed to describe potential difference between the vacuum and the TIQD with R as its radius. The eigenstates of the QD $|\psi_{j,\uparrow\downarrow}\rangle$[25, 26] are linear combinations of degenerate eigenstates of $\hat{J}_z$ which is conserved along the z axis. Note, we refer to $|\psi_{j,\uparrow\downarrow}\rangle$ as spin-up (down) states, as they are the eigenstates for the upper (lower) block of the 4×4 Hamiltonian.

For a given $w_{\uparrow\downarrow}=j\mp1$, the lowest energy state $|w,\uparrow\downarrow\rangle=|\psi_{w\pm1,\uparrow\downarrow}\rangle_{\text{low}}$ with its energy $\epsilon_{w,\uparrow\downarrow}$ in the non-trivial gap $[M,-M]$, is a massless edge state[27, 28]. Here we go beyond Refs. [27, 28] and use winding numbers to classify the edge states: $2w_{\uparrow\downarrow}=(j\mp1/2)+(j\mp3/2)$ is the total winding number in the basis $|e,\uparrow\downarrow\rangle$ and $|hh,\uparrow\downarrow\rangle$ as we will explain below. The edge states localize on the edge and possess a linear energy dispersion $\epsilon_{w,\uparrow\downarrow}=\pm w\cdot\Delta\epsilon+\epsilon_0$. The energy level spacing $\Delta\epsilon=-A[1-(D/B)^2]^{1/2}R^{-1}$[27] depends on QD's radius, and ϵ_0 is the constant sets the Dirac point. $|w,\uparrow\rangle$ and $|-w,\downarrow\rangle=\Theta\,|w,\uparrow\rangle$ are always degenerate due to the TRS. Here $\Theta=-i\sigma_yK$ is a time-reversal operator and K is the operation of complex conjugation. Due to the TRS, the backscattering between $|w,\uparrow\rangle$ and $|-w,\downarrow\rangle$ are

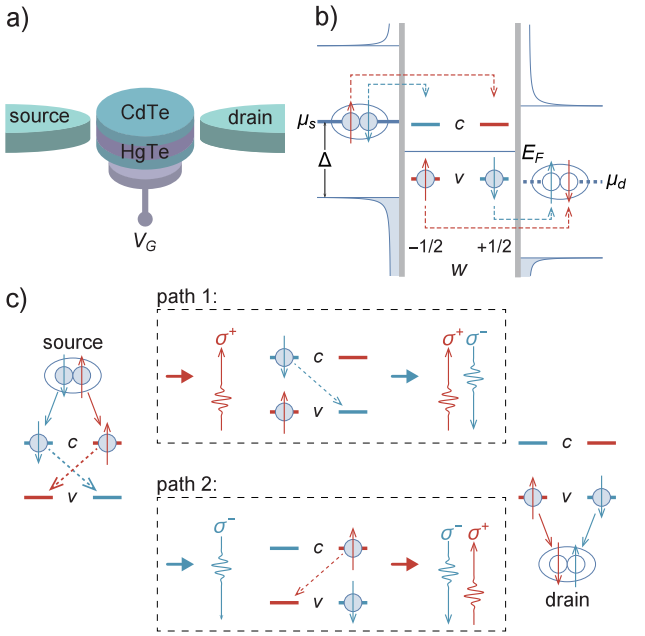

FIG. 1: (color online). (a) Sketch of the proposed p-n junction with SC source and drain electrodes weakly coupled to a HgTe QD whose Fermi level is controlled by a gate electrode V_G. (b) Energy diagram for the structure shown in (a): Δ is the SC gap; μ_s and μ_d are the Fermi energies of the source and drain electrodes; E_F is the Fermi level and c (v) stands for conduction (valance) level we defined in the HgTe QD; Red (blue) bars inside the QD region are spin-up (down) edge states, w denotes their winding numbers; Shaded circles with red (blue) arrows are spin-up (down) electrons; The white circles on the drain side are holes; The ellipses enclose two shaded (white) circles are electron- (hole-) type Cooper pairs; Dashed arrows show the charge transfers from the source to drain electrode through the HgTe QD as electron singlets. The thin grey areas are barriers between the leads and the QD. (c) The initial state of the QD $|2\rangle_c|0\rangle_v$ goes through two indistinguishable pathes with the intermediate state $|\sigma^+\rangle|\downarrow\rangle_c|\uparrow\rangle_v + |\sigma^-\rangle|\uparrow\rangle_c|\downarrow\rangle_v$, and becomes an entangled final state $\left(|\sigma^+\sigma^-\rangle + |\sigma^-\sigma^+\rangle\right)|0\rangle_c|2\rangle_v/\sqrt{2}$. $\sigma^\pm$ is a right-handed (left-handed) circularly polarized photon carrying one unit of angular momentum $\pm\hbar$. Dashed arrows are possible decay pathes.

not allowed, therefore edge states possess a long spin lifetime[29, 30]. The momentum matrix $\mathbf{P} \propto \partial H_{4\times4}/\partial\mathbf{k}$ is block-diagonal and will not couple the spin-up and spin-down states, thus the transition between the edge states with opposite spins is forbidden. For photons propagating in z direction, circular polarized transitions only exist between the states with the same spin while conserving j.

We assume the Fermi energy of the HgTe QD is between two energy levels $\epsilon_c = \epsilon_{\pm1/2,\uparrow\downarrow}$ and $\epsilon_v = \epsilon_{\mp1/2,\uparrow\downarrow}$. They are evenly away from the Dirac point, and the corresponding edge states have an additional TRS symmetry $i\Theta|w,\uparrow\downarrow\rangle = |-w,\uparrow\downarrow\rangle$ because near the Dirac point keeping the linear terms in k one has $K[\sigma_y H_{\uparrow\downarrow}(\hat{\mathbf{k}})\sigma_y \cdot \sigma_y|w,\uparrow\downarrow\rangle] = -H_{\uparrow\downarrow}(\hat{\mathbf{k}})[i\Theta|w,\uparrow\downarrow\rangle] = \epsilon_{w,\uparrow\downarrow}[i\Theta|w,\uparrow\downarrow\rangle]$. We call ϵ_c conduction level and ϵ_v valance level for convenience. $H_\alpha = \epsilon_\alpha \sum_{\sigma=\uparrow\downarrow} a^\dagger_{\alpha,\sigma}a_{\alpha,\sigma} + U_\alpha n_{\alpha,\uparrow}n_{\alpha,\downarrow}$ is the Hamiltonian for the conduction ($\alpha = c$) or valance ($\alpha = v$) level. Two pairs of degenerate edge states are obtained by the creation or annihilation operator: $a^\dagger_{\alpha,\uparrow\downarrow}|0\rangle_c = a_{\alpha,\uparrow\downarrow}|2\rangle_\alpha = |\downarrow\uparrow\rangle_\alpha$, where $|0\rangle_\alpha$ is the empty state and $|2\rangle_\alpha = a^\dagger_{\alpha,\uparrow}a^\dagger_{\alpha,\downarrow}|0\rangle_\alpha$ is the two-electron occupied state for the conduction/valance ($\alpha = c/v$) level. We denote $|\uparrow\downarrow\rangle_c = |\pm1/2,\uparrow\downarrow\rangle$ and $|\uparrow\downarrow\rangle_v = |\mp1/2,\uparrow\downarrow\rangle$ since the spin and angular momentum indices are locked for the corresponding level. We will prove later: 1) when there is one electron in the conduction level and one electron in the valance level, the resulting two-particle states $|\uparrow\rangle_c|\downarrow\rangle_v$ and $|\downarrow\rangle_c|\uparrow\rangle_v$ are degenerate exciton states with the same Coulomb repulsion U between the two electrons due to the TRS; 2) $U_{c,v} = U$ describes the charging energy by electron edge states in the conduction/valance level.

Superconducting p-n junction as a light-emitting diode.— We coupled the HgTe QD weakly to a s-wave SC p-n junction, with pair potential $\Delta_{s,d}$ and chemical potential $\mu_{s,d}$ for its source (drain) lead [see Fig. 1 (b)]. $eV_{sd} = \mu_s - \mu_d$ is the bias voltage applied across the junction. $\mu_{s,d}$ is aligned to the conduction (valance) level $\epsilon_{c,v}$. Once the charge transfers through the p-n junction, biexciton state $|2\rangle_c|0\rangle_v$, which has two electrons in the conduction level and no electron in the valance level, would go through a two-step cascade process [see Fig. 1 (c)]: 1) $|2\rangle_c|0\rangle_v \to |1\rangle_c|1\rangle_v$, the biexciton undergoes a spontaneous transition to $|1\rangle_c|1\rangle_v$, one of the two degenerate exciton states $|\uparrow\rangle_c|\downarrow\rangle_v$ and $|\downarrow\rangle_c|\uparrow\rangle_v$; 2) $|1\rangle_c|1\rangle_v \to |0\rangle_c|2\rangle_v$, the exciton state $|1\rangle_c|1\rangle_v$ decays to $|0\rangle_c|2\rangle_v$. During the cascade, two photons with energy $\hbar\omega_0 \simeq eV_{sd}$, which is in terahertz ($\sim$ meV), are produced. Here we use a waveguide to produce photons propagating along the z axis only[19, 31]. The transition is described by the following Hamiltonian:

$$H_{\rm int} = g\sum_{q_z}\left(\hat{b}^\dagger_{q_z,+}a^\dagger_{v,\uparrow}a_{c,\uparrow} + \hat{b}^\dagger_{q_z,-}a^\dagger_{v,\downarrow}a_{c,\downarrow}\right) + \text{h.c.}, \quad (2)$$

which conserves the J_z, as a right-handed (left-handed) circularly polarized photon $\hat{b}^\dagger_{q_z,\pm}|0\rangle = |\sigma^\pm\rangle$ conveys one unit of angular momentum $\pm\hbar$. The coupling strength $g \sim e(\hbar\omega_0/2\epsilon V)^{1/2}$ can be tuned by changing the volume of the waveguide. After each biexciton cascade, the final two-photon state entangled with opposite circular polarizations is

$$|\psi\rangle = \left(|\sigma^+\sigma^-\rangle + |\sigma^-\sigma^+\rangle\right)/\sqrt{2}. \quad (3)$$

This final state means the two sequentially produced photons in the z direction are polarization entangled: if the first emitted photon is σ^+ (σ^-), then the second emitted photon is σ^- (σ^+). For a HgTe QD with a radius $R = 150$nm, both the biased voltage $eV_{sd} \simeq 2.4$meV and

the charging energy $U \simeq 0.8$meV[28] are smaller than $\Delta_{s,d} \approx 3$meV (for Nb). In this case, we neglect the transitions creating a single quasiparticle in the SC leads. The emission intensity of circular polarization entangled photons equals to charge current through the junction.

The weak coupling between the HgTe QD and the SC leads will slightly split the energy levels for two-particle states $|2\rangle_c|0\rangle_v$ and $|0\rangle_c|2\rangle_v$ and shifts the frequencies of emitted photons from the central frequency ω_0[12, 26]. However, edge states and exciton states in the HgTe QD is unaffected by this weak coupling, and the polarizations and energies of the photons are uncorrelated. The delay time τ_X between the first and second emission events is much shorter than the emission time of the pair τ_{XX} ($\tau_X/\tau_{XX} \sim 0.09$)[12], thus the two photons in a pair are time- and polarization-correlated. In our proposal, the SC gaps forbid single quasiparticle creation in the SC leads, so the entangled photons are produced pair by pair and could be identified efficiently in the time domain. This pair-by-pair feature could also appear in a large non-trivial gap (about 0.3eV) TIQD[32] with the aid of the Pauli exclusion principle[4].

Superradiance and Josephson effect has been discussed in similar SC p-n systems[12, 33]. Here we neglect these effects because the absence of a static in-plane electric field does not allow the emission of a single photon from Cooper pair transfer through the QD via Josephson effect[12]. Our proposal is based on the biexciton cascade process which is not related to the Josephson effect.

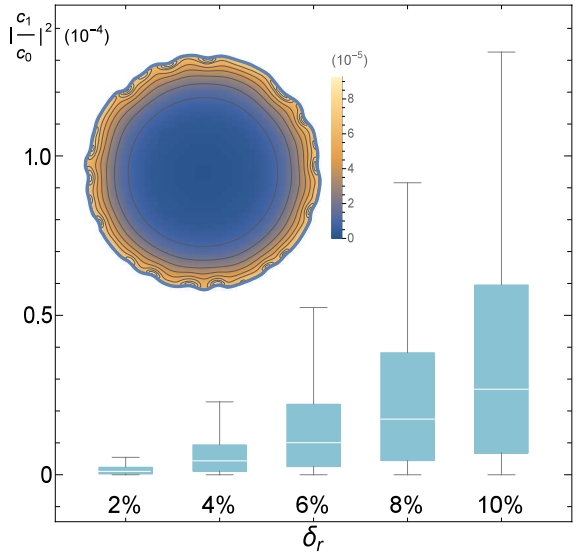

FIG. 2: (color online). Calculated $|c_1/c_0|^2$ for 10^3 TIQDs using finite element method. The TIQDs are generated by fluctuating their radius randomly as $r_0[1+\delta_r f(\theta)]$ in the polar coordinate system; $r_0 = 150$nm, $f(\theta) \in [-1, 1]$ is a random function. The results are classified by δ_r which denotes the maximum fluctuation percentage. The inset shows the density distributions of an edge state in one of the randomly shaped TIQDs.

Zero FSS in generic TIQDs.— We now prove in generic TIQDs, two-particle states $|\uparrow\rangle_c|\downarrow\rangle_v$ and $|\downarrow\rangle_c|\uparrow\rangle_v$ are degenerate exciton states without FSS. $|\uparrow\rangle_c|\downarrow\rangle_v$ and $|\downarrow\rangle_c|\uparrow\rangle_v$ are products of edge states which satisfy: 1) $|\downarrow\rangle_\alpha = |\Theta\uparrow\rangle_\alpha$ ($\alpha = c, v$) due to the TRS; 2) more specifically, an additional TRS symmetry $|\uparrow\downarrow\rangle_c = i\Theta|\uparrow\downarrow\rangle_v$ near the Dirac point. These two relations hold, not only for HgTe QDs, but also for generic TIQDs that are composed of other materials.

The two-particle Hamiltonian for the conduction and valance level is $H_{cv} = \sum_{\alpha=c,v}\sum_{\sigma=\uparrow\downarrow}\epsilon_\alpha a^\dagger_{\alpha,\sigma}a_{\alpha,\sigma} + \hat{V}$, where $\hat{V}$ is the Coulomb interaction between the two electrons. The bright exciton states must be the linear combinations of the two-particle states $|\uparrow\rangle_c|\downarrow\rangle_v$ and $|\downarrow\rangle_c|\uparrow\rangle_v$[26]. In the basis $\{|\uparrow\rangle_c|\downarrow\rangle_v, |\downarrow\rangle_c|\uparrow\rangle_v\}$, the off-diagonal term of H_{cv} is $\langle\uparrow|_c\langle\downarrow|_v H_{cv}|\downarrow\rangle_c|\uparrow\rangle_v = \langle\uparrow|_c\langle\downarrow|_v\hat{V}|\downarrow\rangle_c|\uparrow\rangle_v = 0$[26] as $\hat{V}$ commutes with the time-reversal operator $\Theta^2 = -1$. Two diagonal terms are also the same as $\langle\uparrow|_c\langle\downarrow|_v\hat{V}|\uparrow\rangle_c|\downarrow\rangle_v = \langle\downarrow|_c\langle\uparrow|_v\hat{V}|\downarrow\rangle_c|\uparrow\rangle_v \equiv U$. Therefore $|\uparrow\rangle_c|\downarrow\rangle_v$ and $|\downarrow\rangle_c|\uparrow\rangle_v$ are degenerate exciton states with the same energy $\epsilon_c + \epsilon_v + U$. Besides, $U_\alpha = \langle\uparrow|_\alpha\langle\downarrow|_\alpha\hat{V}|\uparrow\rangle_\alpha|\downarrow\rangle_\alpha = U$ ($\alpha = c, v$)[26].

On the other side, the exciton FSS arises from the exchange interaction between two exciton states. Note that, by swapping its electron with the hole, $|\uparrow\rangle_c|\downarrow\rangle_v$ is transformed to $|\downarrow\rangle_c|\uparrow\rangle_v$. The exchange energy[34] $E_{ex} \propto \langle\uparrow|_c\langle\downarrow|_v\hat{V}|\downarrow\rangle_c|\uparrow\rangle_v = 0$ leads to vanishing FSS between the two exciton states. The physical reason behind the zero FSS is that the backscattering is forbidden by TRS. It is necessary to emphasize that, the unavoidable non-magnetic disorders and morphology variations of a TIQD will not break TRS. Therefore the FSS vanishes between exciton states $|\uparrow\rangle_c|\downarrow\rangle_v$ and $|\downarrow\rangle_c|\uparrow\rangle_v$ in generic TIQDs as long as the TRS symmetry exist. This is the significance between the TIQDs and the conventional semiconductor QDs studied before.

Winding number conservation.— One may intuitively conclude $SO(2)$ symmetry in an actual TIQD will be broken, so that J_z is not conserved and the original selection rules do not hold. Therefore, the final photon state $|\psi'\rangle = c_0(|\sigma^+\sigma^-\rangle + |\sigma^-\sigma^+\rangle)/\sqrt{2} + c_1(|\sigma^+\sigma^+\rangle + |\sigma^-\sigma^-\rangle)/\sqrt{2}$ with $|c_0|^2 + |c_1|^2 = 1$ possesses the reduced fidelity $\mathcal{F} = [1+|c_1/c_0|^2]^{-1}$ with respect to Bell state. To quantitatively analyze the magnitude of $|c_1/c_0|^2$, we have performed finite element method simulations[26] on about 10^3 different HgTe QDs with random shapes. We generate these QDs by fluctuating their boundaries as $r(\theta) = r_0[1+\delta_r f(\theta)]$ in the polar coordinate system, where the mean radius is $r_0 = \int_0^{2\pi} r(\theta)\,d\theta/2\pi$ while the random function $f(\theta) \in [-1, 1]$ satisfies $f(\theta) = f(\theta + 2\pi)$, where δ_r is a dimensionless number characterizing the maximum fluctuation percentage (typically less than 10% in experiments). The simulation results (see Fig. 2) show that the irregularities of the TIQDs' configurations only cause neglectable deviations ($\lesssim 10^{-4}$) of selection rules

from that with a perfect circular shape.

We have a topological explanation for this robustness of selection rules against randomness of the TIQDs' morphologies. Consider a 1D system on a closed loop with *linear* dispersion (see Fig. 3). The Hamiltonian for the

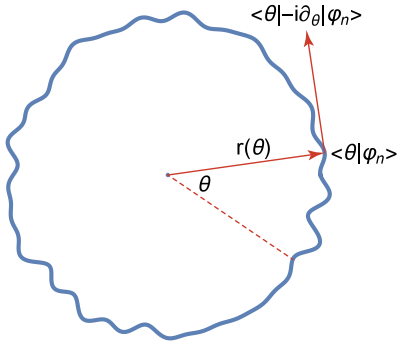

FIG. 3: (color online). A 1D system on a closed loop with linear dispersion. $\langle\varphi_n|\,\hat{k}_\theta\,|\varphi_n\rangle$ is the winding number counting the total number of counterclockwise turns that $|\varphi_n\rangle$ makes around the origin.

system reads $\hat{H}=\Delta\epsilon\cdot\hat{k}_\theta+V(\theta)$ and depends on a single parameter $\theta\in[0,2\pi]$. Both the variations of the radius $r(\theta)$ and the disorder potential $V(\theta)$ break $SO(2)$ symmetry. Although J_z is no longer conserved, eigenstate of the system $\langle\theta|\varphi_n\rangle=\exp[i\phi_n(\theta)]/\sqrt{2\pi}$ with energy $n\cdot\Delta\epsilon+\epsilon_0$ has a well defined winding number

$$w_n=\int_0^{2\pi}\langle\varphi_n|\theta\rangle\langle\theta|-i\partial_\theta|\varphi_n\rangle=n, \tag{4}$$

because its phase term $\phi_n(\theta)=n\theta+\delta(\theta)$ must satisfy $\phi_n(\theta+2\pi)=\phi_n(\theta)+2\pi n$ $(n\in\mathbb{Z})$ to match the periodical boundary condition. The phase-shift term $\delta(\theta)=[\epsilon_0\theta+\int_0^\theta V(\theta')\,\mathrm{d}\theta']/\Delta\epsilon$ with $\delta(2\pi)=0$ is independent of n, which is possible only for a massless 1D system. The winding number characterize the total number of counterclockwise turns that the wavefunction makes around the origin. The coupling between eigenstates $|\varphi_n\rangle$ and $|\varphi_{n'}\rangle$ with different *winding numbers* n and n' by circularly polarized photon with angular momentum ±1 is proportional to

$$\begin{aligned}C^{\pm}_{n,n'}&=\langle\varphi_n|\,\hat{r}_\pm\,|\varphi_{n'}\rangle=\int_0^{2\pi}\langle\varphi_n|\theta\rangle\,r(\theta)\,e^{\pm i\theta}\,\langle\theta|\varphi_{n'}\rangle\\&=r_0\delta_{n,n'\pm1}+r_0\delta_r\int_0^{2\pi}f(\theta)\,e^{i(-n+n'\pm1)\theta}\mathrm{d}\theta/2\pi.\end{aligned} \tag{5}$$

The second term of $C^{\pm}_{n,n'}$ vanishes when $n=n'\pm1$ because $\int_0^{2\pi}f(\theta)\,\mathrm{d}\theta/2\pi=0$. It can be neglected when $n\neq n'\pm1$ because $\int_0^{2\pi}f(\theta)\exp[i(-n+n'\pm1)\theta]\mathrm{d}\theta/2\pi=f_{n'\pm1-n}$ is the $(n'\pm1-n)$th Fourier coefficient of $f(\theta)$, and $|f_{n'\pm1-n}|\ll1$ for a random fluctuation[35]. Therefore the selection rules for circularly polarized photons in this system respect winding number conservation $n=n'\pm1$. On the other hand, the edge states in a TIQD are naturally quasi 1D states (see inset in Fig. 2) with linear dispersions regardless of the TIQD's shape due to their massless feature, which also originates from the topological property of the TIQD[29, 30]. The winding number for each of the edge states in a specific basis, e.g., $\{|e,\uparrow\downarrow\rangle,|hh,\uparrow\downarrow\rangle\}$, is well defined. Therefore the selection rules between edge states in TIQDs respect the conservation of the topological winding number. The zero FSS together with the winding number conservation during the cascade process in TIQDs results in the final two-photon state, whose entanglement is robust against disorders, morphology fluctuations and asymmetry of the TIQD.

Conclusion.— In this Letter, we proposed a realizable scheme to produce photon pairs at terahertz regime with robust entanglement in generic topological insulator quantum dots (TIQDs). We prove one-dimensional massless excitons composed of edge states with linear dispersions in TIQDs are free from the fine structure splitting (FSS) due to the time-reversal symmetry. The entanglement of the emitted photon pairs from the cascade process is robust against disorders and morphology fluctuations in TIQDs, because of the absence of FSS and the selection rules between edge states respecting the winding number conservation. Both merits root in the topology of the proposed TIQD. These two findings have *not* been discussed in previous literatures as far as we know. Note that our results are valid near the Dirac point where the dispersions of edge states are linear. This discovery paves a new way towards the future applications and integrations of entangled photon pair emitters, and possible novel optical devices based on winding number conservation, by utilizing the massless edge states of topological materials. Our scheme, which can be implemented using current experimental techniques, is free from the requirements to fabricate quantum dots with high symmetry and sophisticated regulations to eliminate FSS.

K.C. is supported by NSFC Grants No.11434010 and the Grant Nos. 2015CB921503, and 2011CB922204-2 from the MOST of China. C.-P. S. acknowledges support from the NSFC Grant Nos. 11421063 and 11534002, and the National 973 program (Grant Nos. 2012CB922104 and 2014CB921403).

[1] C. H. Bennet and G. Brassard, in *IEEE International Conference on Computers, Systems and Signal Processing* (IEEE, New York, 1984).
[2] A. K. Ekert, Phys. Rev. Lett. **67**, 661 (1991).
[3] C. H. Bennett, G. Brassard, C. Crépeau, R. Jozsa, A. Peres, and W. K. Wootters, Phys. Rev. Lett. **70**, 1895 (1993).
[4] O. Benson, C. Santori, M. Pelton, and Y. Yamamoto, Phys. Rev. Lett. **84**, 2513 (2000).

[5] R. M. Stevenson, R. J. Young, P. Atkinson, K. Cooper, D. A. Ritchie and A. J. Shields, Nature **439**, 179 (2006).

[6] R. J Young, R M. Stevenson, P. Atkinson, K. Cooper, D. A. Ritchie and A. J. Shields, New J. Phys. **8**, 29 (2006).

[7] N. Akopian, N. H. Lindner, E. Poem, Y. Berlatzky, J. Avron, D. Gershoni, B. D. Gerardot, and P. M. Petroff, Phys. Rev. Lett. **96**, 130501 (2006).

[8] A. J. Hudson, R. M. Stevenson, A. J. Bennett, R. J. Young, C. A. Nicoll, P. Atkinson, K. Cooper, D. A. Ritchie, and A. J. Shields, Phys. Rev. Lett. **99**, 266802 (2007).

[9] R. Singh and G. Bester, Phys. Rev. Lett. **103**, 063601 (2009).

[10] A. Schliwa, M. Winkelnkemper, A. Lochmann, E. Stock, and D. Bimberg, Phys. Rev. B **80**, 161307(R) (2009).

[11] C. L. Salter, R. M. Stevenson, I. Farrer, C. A. Nicoll, D. A. Ritchie and A. J. Shields, Nature **465**, 594 (2010).

[12] P. Recher, Y. V. Nazarov, and L. P. Kouwenhoven, Phys. Rev. Lett. **104**, 156802 (2010).

[13] A. J. Bennett, M. A. Pooley, R. M. Stevenson, M. B. Ward,R. B. Patel, A. Boyer de la Giroday, N. Sköld, I. Farrer,C. A. Nicoll, D. A. Ritchie, and A. J. Shields, Nature Phys. **6**, 947 (2010).

[14] A. Mohan, M. Felici, P. Gallo, B. Dwir, A. Rudra, J. Faist and E. Kapon, Nat. Photon. **4**, 302 (2010).

[15] C. E. Kuklewicz, R. N. E. Malein, P. M. Petroff, and B. D. Gerardot, Nano Lett. **12**, 3761 (2012).

[16] R. Trotta, E. Zallo, C. Ortix, P. Atkinson, J. D. Plumhof, J. van den Brink, A. Rastelli, and O. G. Schmidt, Phys. Rev. Lett. **109**, 147401 (2012).

[17] G. Juska, V. Dimastrodonato, L. O. Mereni, A. Gocalinska, and E. Pelucchi, Nat. Photon. **7**, 527 (2013).

[18] M. Müller, S. Bounouar, K. D. Jöns, M. Glässl and P. Michler, Nat. Photon. **8**, 224 (2014).

[19] Marijn A. M. Versteegh, M. E. Reimer, K. D. Jöns, D. Dalacu, P. J. Poole, A. Gulinatti, A. Giudice and V. Zwiller, Nat. Commun. **5**, 5298 (2014).

[20] R. Trotta, J. Martín-Sánchez, I. Daruka, C. Ortix, and A. Rastelli, Phys. Rev. Lett. **114**, 150502 (2015).

[21] J. P. Wang, M. Gong, G.-C. Guo, and L. X. He, Phys. Rev. Lett. **115**, 067401 (2015).

[22] S. De Franceschi, L. Kouwenhoven, C. Schönenberger and W. Wernsdorfer, Nat. Nanotech. **5**, 703 (2010).

[23] B. A. Bernevig, T. L. Hughes, and S. C. Zhang, Science **314**, 1757 (2006).

[24] The Four-band Hamiltonian describes the low energy electron dynamics, which is derived from the full multi-band Hamiltonian with strong spin-orbit coupling and band mixing effects included. The inversion of the band gap, i.e., $M > 0$ to $M < 0$ transition, is the major result of the strong spin-orbit coupling. *hh* indicate not exactly but largely heavy hole bands, as other hole bands are absorbed into the heavy hole bands during the Hamiltonian reduction.

[25] E. Tsitsishvili, G. S. Lozano, and A. O. Gogolin, Phys. Rev. B **70**, 115316 (2004).

[26] See Supplemental Material at [URL will be inserted by publisher], which includes Refs. [12], for details of eigenstates in a circular HgTe QD, emissions in the superconducting *p*-*n* junction, Coulomb interactions between two-particle states and notes for our finite element method simulations.

[27] Kai Chang and W. K. Lou, Phys. Rev. Lett. **106**, 206802 (2011).

[28] J. Li, W. K. Lou, D. Zhang, X. J. Li, W. Yang, and Kai Chang, Phys. Rev. B **90**, 115303 (2014).

[29] M. Z. Hasan and C. L. Kane, Rev. Mod. Phys. **82**. 3045 (2010).

[30] X. L. Qi and S. C. Zhang, Rev. Mod. Phys. **83**. 1057 (2011).

[31] K. Wang and D. M. Mittleman, Nature **432**, 376 (2004).

[32] Y. Xu, B. H. Yan, H. J. Zhang, J. Wang, G. Xu, P. Z. Tang, W. H. Duan, and S. C. Zhang, Phys. Rev. Lett. **111**, 136804 (2013).

[33] Y. Asano, I. Suemune, H. Takayanagi, and E. Hanamura, Phys. Rev. Lett. **103**, 187001 (2009).

[34] M. Bayer, G. Ortner, O. Stern, A. Kuther, A. A. Gorbunov, and A. Forchel, Phys. Rev. B **65**, 195315 (2002).

[35] It is reasonable to model the fluctuation of a QD's boundary $f(\theta)$ as the white noise. Because when someone tries to obtain a QD in circular shape by etching, the boundary of the QD is formed by atomic dissociation process which is mesoscopically regulated and microscopically random. Norms of its Fourier coefficients $|f_m| \sim \omega_c^{-1/2}$, where $\omega_c \sim 2\pi r_0/a_0$ is the cut-off frequency of the fluctuation, with r_0 the radius of the QD and a_0 the atomic spacing. For realistic QDs, $2\pi r_0/a_0 > 10^3$, $|f_m|^2 < 10^{-3}$, and $|c_1/c_0|^2 \sim \delta_r^2 |f_m|^2 < 10^{-4}$.

arXiv:1601.04722v3 [cond-mat.mes-hall] 1 Feb 2016

Supplementary Material: Entangled Terahertz Photon Emission from Topological Insulator Quantum Dots

Li-kun Shi,[1] Kai Chang,[2] and Chang-Pu Sun[1]
[1]*Beijing Computational Science Research Center, Beijing 100193, China*
[2]*SKLSM, Institute of Semiconductors, Chinese Academy of Sciences, P.O. Box 912, Beijing 100083, China*

I. Eigenstates in a Circular HgTe Quantum Dot

The low-energy electron states in the HgTe QD are described by a four-band effective Hamiltonian in the basis $|e,\uparrow\rangle$, $|hh,\uparrow\rangle$, $|e,\downarrow\rangle$, and $|hh,\downarrow\rangle$:

$$H_{4\times4}=\begin{bmatrix} H_{\uparrow}(\hat{\mathbf{k}}) & 0 \\ 0 & H_{\downarrow}(\hat{\mathbf{k}}) \end{bmatrix}+V(r), \tag{1-1}$$

where $\hat{\mathbf{k}}=(\hat{k}_x,\hat{k}_y)$ is the in-plane wavevector, $H_{\uparrow}(\hat{\mathbf{k}})=H_{\downarrow}^{*}(-\hat{\mathbf{k}})=\epsilon(\hat{k})I_{2\times2}+d_i(\hat{\mathbf{k}})\sigma^i$, and $\sigma^i\,(i=1,2,3)$ are the Pauli matrices; $\epsilon(\hat{k})=C-D\hat{k}^2$, $d_{1,2}(\hat{\mathbf{k}})=A\hat{k}_{x,y}$, and $d_3(\hat{k})=M-B\hat{k}^2$. The hard-wall confining potential $V(r)$ is employed to describe potential difference between the vacuum and the TIQD with R as its radius. The four-band Hamiltonian is derived from the full multi-band Hamiltonian with strong spin-orbit coupling and band mixing effects included. The total angular momentum $\hat{J}_{z,\uparrow\downarrow}=\hat{L}_z+\hat{S}_{z,\uparrow\downarrow}$, where $\hat{L}_z$ is the orbit azimuthal angular momentum, and $\hat{S}_{z,\uparrow\downarrow}$ is the spin projection onto the z direction, which is $\pm1/2$ for $|e,\uparrow\downarrow\rangle$ and $\pm3/2$ for $|hh,\uparrow\downarrow\rangle$. One can verify $[H_{\uparrow\downarrow},\hat{J}_{z,\uparrow\downarrow}]=0$.

The eigenstate of $\hat{J}_z$ in the basis $\{|e,\uparrow\rangle,|hh,\uparrow\rangle,|e,\downarrow\rangle,|hh,\downarrow\rangle\}$ satisfying $\hat{J}_{z,,\uparrow\downarrow}|\psi_{j,\uparrow\downarrow}\rangle=j|\psi_{j,\uparrow\downarrow}\rangle$ has the form

$$\psi_{j,\uparrow\downarrow}(r,\phi)=\{c_{1,\uparrow\downarrow}J_{j-1/2}(kr)\exp[i(j\mp1/2)\phi],c_{2,\uparrow\downarrow}J_{j-3/2}(kr)\exp[i(j\mp3/2)\phi]\}^T \tag{1-2}$$

in the polar coordinate. For bulk states with no boundary constraints on k, the eigenequation is $\hat{H}_{\uparrow\downarrow}|\psi_{j,\uparrow\downarrow}\rangle=\epsilon|\psi_{j,\uparrow\downarrow}\rangle$, which leads to $\mathcal{M}_{1,\uparrow\downarrow}[c_{1,\uparrow\downarrow},c_{2,\uparrow\downarrow}]^T=0$ and the relation between k and ϵ:

$$\det\mathcal{M}_{1,\uparrow\downarrow}=0, \tag{1-3}$$

where

$$\mathcal{M}_{1,\uparrow\downarrow}=\begin{bmatrix} M-B_+k^2-\epsilon & \mp iAk \\ \pm iAk & -M+B_-k^2-\epsilon \end{bmatrix}. \tag{1-4}$$

As the bulk spectrum has two branches, for a given value of ϵ there are two non-trivial solutions k_i $(i=1,2)$ for the momentum. For eigenstates in the QD, we are able to satisfy their vanishing boundary condition $\psi_{j,\uparrow\downarrow}(R)=0$ by combining two linearly independent degenerate solutions in the bulk $\psi_{j,\uparrow\downarrow}(r)=\sum_{i=1}^{2}[c_{1i,\uparrow\downarrow}J_{j\mp1/2}(k_ir),c_{2i,\uparrow\downarrow}J_{j\mp3/2}(k_ir)]^T$ and requiring the coefficients to satisfy $\mathcal{M}_{1,\uparrow\downarrow}[c_{1i,\uparrow\downarrow},c_{2i,\uparrow\downarrow}]^T=0$. For convenience we define $\gamma_{2i,\uparrow\downarrow}$ as

$$\gamma_{2i,\uparrow\downarrow}=c_{2i,\uparrow\downarrow}/c_{1i,\uparrow\downarrow}=\pm iAk_i/(-M+B_-k_i^2-\epsilon). \tag{1-5}$$

Therefore

$$\psi_{j,\uparrow\downarrow}(r)=\sum_{i=1}^{2}c_{1i,\uparrow\downarrow}[J_{j\mp1/2}(k_ir),\gamma_{2i,\uparrow\downarrow}J_{j\mp3/2}(k_ir)]^T, \tag{1-6}$$

then $\psi_{j,\uparrow\downarrow}(R)=0$ leads to $\mathcal{M}_{2,\uparrow\downarrow}[c_{11,\uparrow\downarrow},c_{12,\uparrow\downarrow}]^T=0$ and the equation to fix the eigenenergy:

$$\det\mathcal{M}_{2,\uparrow\downarrow}=0, \tag{1-7}$$

where

$$\mathcal{M}_2=\begin{bmatrix} J_{j\mp1/2}(k_1R) & J_{j\mp1/2}(k_2R) \\ \gamma_{21,\uparrow\downarrow}J_{j\mp3/2}(k_1R) & \gamma_{22,\uparrow\downarrow}J_{j\mp3/2}(k_2R) \end{bmatrix}. \tag{1-8}$$

II. Emissions from the Superconducting p-n Junction

The weak coupling between the QD and the SC leads induce a pair potential $\Delta_{c,v} = \exp[i\phi_{\rm s,d}]\Gamma_{\rm s,d}/2$ for the conduction (valance) level, i.e., the proximity effect. $\phi_{\rm s,d}$ is the phase of the corresponding $\Delta_{\rm s,d}$, and $\Gamma_{\rm s,d}$ characterize the broadening of the conduction (valance) level proportional to square of the tunneling amplitude (assuming $\Gamma_{\rm s,d} \ll |\Delta_{\rm s,d}|$, i.e., the coupling between the QD and SC leads is weak). The effective low-energy Hamiltonian for the conduction ($\alpha = c$) or valance ($\alpha = v$) level is

$$\begin{aligned}\tilde{H}_\alpha = \tilde{\epsilon}_\alpha \sum_{\sigma=\uparrow\downarrow} a^\dagger_{\alpha,\sigma} a_{\alpha,\sigma} + U n_{\alpha,\uparrow} n_{\alpha,\downarrow} \\ + \Delta_\alpha a^\dagger_{\alpha,\uparrow} a^\dagger_{\alpha,\downarrow} + \Delta^*_\alpha a_{\alpha,\downarrow} a_{\alpha,\uparrow},\end{aligned} \tag{2-1}$$

where $\tilde{\epsilon}_{c,v} = \epsilon_{c,v} - \mu_{\rm s,d}$ counts from $\mu_{\rm s,d}$. By diagonalizing $\tilde{H}_\alpha$, beside two degenerate states $a^\dagger_{\alpha,\uparrow\downarrow}|0\rangle_\alpha$ with energy $\tilde{\epsilon}_\alpha$, there are excited and ground states being linear superposition of empty state $|0\rangle_\alpha$ and fully occupied two-particle state $|2\rangle_\alpha$, i.e.,

$$|\pm\rangle_\alpha = -\exp[-i\phi_\alpha]\,|u_{\alpha,\pm}|\,|0\rangle_\alpha + |u_{\alpha,\mp}|\,|2\rangle_\alpha\,, \tag{2-2}$$

with

$$\tilde{\epsilon}_{\alpha,\pm} = \varepsilon_\alpha \pm (\varepsilon^2_\alpha + |\Delta_\alpha|^2)^{1/2}, \tag{2-3}$$

where $\varepsilon_\alpha = \tilde{\epsilon}_\alpha + U/2$ and $|u_{\alpha,\pm}| = (1/\sqrt{2}) \times [1 \pm \varepsilon_\alpha/(\varepsilon^2_\alpha + |\Delta_\alpha|^2)^{1/2}]^{1/2}$.

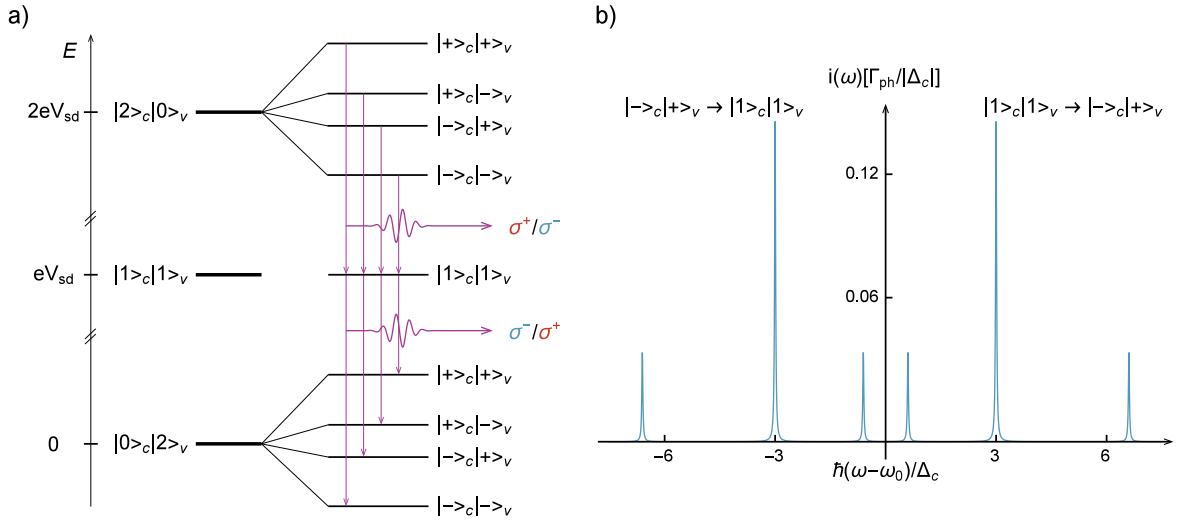

FIG. 1: (a) Sketch of the energy level splittings for two-particle states in the HgTe QD weakly coupled to SC electrodes. The p-n junction is biased with a voltage $V_{\rm s,d}$. The cascade produces two photons with opposite circular polarization $\sigma^\pm$. (b) Emission intensity of time- and polarization-correlated photons emitted from the biexciton cascade. The central frequency $\hbar\omega_0 \simeq eV_{\rm sd}$. The dominant cascade process is $|-\rangle_c|+\rangle_v \to |1\rangle_c|1\rangle_v \to |-\rangle_c|+\rangle_v$. Parameters: $\tilde{\epsilon}_c = \tilde{\epsilon}_v = 0$, $U = 3$, $\Gamma_{\rm ph} = 0.02$ (in units of $\Delta_c = \Delta_v$).

The emission intensity computed versus photon frequency ω is shown in Fig. 1 (b). The emission intensity is $i(\omega_{q_z}) = \sum_{ab,p} w^p_{a\to b}(\omega_{q_z})\,\rho_a$ with the transition rate $w^p_{a\to b}(\omega_{q_z}) = (2\pi/\hbar)\sum_{q_z} |\langle b; q_z, p\,|H_{\rm int}|\,a; 0\rangle|^2\,\delta[\tilde{\epsilon}_{ab} - \hbar\tilde{\omega}_{q_z} + i\Gamma_{\rm ph}]$. We will explain below the symbols in $i(\omega_{q_z})$ and $w^p_{a\to b}(\omega_{q_z})$:

a, b are one of six possible states in the QD $\{|+\rangle_c|+\rangle_v,\ |+\rangle_c|-\rangle_v,\ |-\rangle_c|+\rangle_v,\ |-\rangle_c|-\rangle_v,\ |\uparrow\rangle_c|\downarrow\rangle_v,\ |\downarrow\rangle_c|\uparrow\rangle_v\}$ [see Fig. 1 (a)]. These six states are direct products of two eigenstates (one from the conduction level and another one from the valance level) and can always be expanded by in the basis $\{|2\rangle_c|2\rangle_v, |0\rangle_c|0\rangle_v, |2\rangle_c|0\rangle_v, |0\rangle_c|2\rangle_v, |\uparrow\rangle_c|\downarrow\rangle_v, |\downarrow\rangle_c|\uparrow\rangle_v\}$. In our work we only use electron notations and do not introduce hole operators. For example, $|2\rangle_c|0\rangle_v$ means there are two electrons in the conduction level and no electron in the valance level (biexciton); $|1\rangle_c|1\rangle_v$ means there is one electron in the conduction level and one electron in the valance level (exciton); $|0\rangle_c|2\rangle_v$ means there is no electron in the conduction level and two electrons in the valance level (no exciton).

$p=\sigma^{\pm}$ denotes the polarization; $\tilde{\epsilon}_{ab}=\tilde{\epsilon}_a-\tilde{\epsilon}_b$ is the energy difference between states a and b (Note that $\tilde{\epsilon}_a$ or $\tilde{\epsilon}_b$ is the energy for *two-particle* state); $\tilde{\omega}_{q_z}=\omega_{q_z}-\omega_0$ is the frequency shift caused by proximity effect; and $\Gamma_{\rm ph}=2\pi\nu_{\rm ph}\left|g\right|^2$ is the broadening of the emission peaks with $\nu_{\rm ph}$ the photon DOS assumed to be independent of energy and polarization. The probabilities ρ_a are determined by the stationary solution of the master equation $\dot{\rho}_a=\sum_{b,p}[W^p_{b\to a}\rho_b-W^p_{a\to b}\rho_a]$, $W^p_{a\to b}=\int \mathrm{d}\omega' w^p_{a\to b}\left(\omega'\right)$.

At the first glance, it is weird to see the initial state of the QD is the same with the final state after biexciton cascade. In fact, the state $\left|-\right\rangle_c\left|+\right\rangle_v$ is the superposition of two parts: $\left|2\right\rangle_c\left|0\right\rangle_v$ with two electrons in the conduction level and $\left|0\right\rangle_c\left|2\right\rangle_v$ with two electrons in the valance level. Therefore the initial state is actually the $\left|2\right\rangle_c\left|0\right\rangle_v$ part of the $\left|-\right\rangle_c\left|+\right\rangle_v$ and the final state is the $\left|0\right\rangle_c\left|2\right\rangle_v$ part of the $\left|-\right\rangle_c\left|+\right\rangle_v$. However, with induced pair potential $\Delta_{c,v}$, $\left|2\right\rangle_c\left|0\right\rangle_v$ and $\left|0\right\rangle_c\left|2\right\rangle_v$ are no longer two-particle eigenstates. One has to calculate the process like $\left|-\right\rangle_c\left|+\right\rangle_v\to\left|1\right\rangle_c\left|1\right\rangle_v\to\left|-\right\rangle_c\left|+\right\rangle_v$ instead of $\left|2\right\rangle_c\left|0\right\rangle_v\to\left|1\right\rangle_c\left|1\right\rangle_v\to\left|0\right\rangle_c\left|2\right\rangle_v$, while the frequencies of the emitter photons are shifted from the central frequency $\hbar\omega_0=(2\epsilon_c+U)-(\epsilon_c+\epsilon_v+U)=(\epsilon_c+\epsilon_v+U)-(2\epsilon_v+U)=\epsilon_c-\epsilon_v=\mathrm{e}V_{\rm sd}$, where $2\epsilon_c+U$ is the energy for $\left|2\right\rangle_c\left|0\right\rangle_v$ state; $2\epsilon_v+U$ is the energy for $\left|2\right\rangle_c\left|0\right\rangle_v$ state; $(\epsilon_c+\epsilon_v+U)$ is the energy for $\left|1\right\rangle_c\left|1\right\rangle_v$ state.

III. Coulomb Interactions between Two Particle States

The two-particle Hamiltonian for the conduction and valance level is

$$H_{cv}=\sum_{\alpha=c,v}\sum_{\sigma=\uparrow\downarrow}\epsilon_\alpha a^\dagger_{\alpha,\sigma}a_{\alpha,\sigma}+\hat{V}, \tag{3-1}$$

where $\hat{V}$ is the Coulomb interaction between the two electrons. Any exciton state must be the linear combinations of the two-particle basis $\{\left|\uparrow\right\rangle_c\left|\downarrow\right\rangle_v,\left|\downarrow\right\rangle_c\left|\uparrow\right\rangle_v,\left|\uparrow\right\rangle_c\left|\uparrow\right\rangle_v,\left|\downarrow\right\rangle_c\left|\downarrow\right\rangle_v\}$, in which one electron is in the conduction level and another in the valance level. These two-particle states are products of edge states which satisfy: 1) $\left|\downarrow\right\rangle_\alpha=\left|\Theta\uparrow\right\rangle_\alpha$ $(\alpha=c,v)$ due to the TRS; 2) an additional symmetry $\left|\uparrow\downarrow\right\rangle_c=i\Theta\left|\uparrow\downarrow\right\rangle_v$ as the conduction and valance level are evenly away from and near the Dirac point. These two relations hold, not only for HgTe QDs, but also for generic TIQDs that are composed of other materials and can have irregular shapes.

In the two-particle basis $\{\left|\uparrow\right\rangle_c\left|\downarrow\right\rangle_v,\left|\downarrow\right\rangle_c\left|\uparrow\right\rangle_v,\left|\uparrow\right\rangle_c\left|\uparrow\right\rangle_v,\left|\downarrow\right\rangle_c\left|\downarrow\right\rangle_v\}$,

$$H_{cv}=\begin{bmatrix}\epsilon_c+\epsilon_v+U & 0 & 0 & 0\\ 0 & \epsilon_c+\epsilon_v+U & 0 & 0\\ 0 & 0 & \epsilon_c+\epsilon_v+U' & \left\langle\uparrow\right|_c\left\langle\uparrow\right|_v\hat{V}\left|\downarrow\right\rangle_c\left|\downarrow\right\rangle_v\\ 0 & 0 & \left\langle\downarrow\right|_c\left\langle\downarrow\right|_v\hat{V}\left|\uparrow\right\rangle_c\left|\uparrow\right\rangle_v & \epsilon_c+\epsilon_v+U'\end{bmatrix}, \tag{3-2}$$

where

$$\begin{aligned}U&=\left\langle\uparrow\right|_c\left\langle\downarrow\right|_v\hat{V}\left|\uparrow\right\rangle_c\left|\downarrow\right\rangle_v=\left\langle\Theta\downarrow\right|_c\left\langle-\Theta\uparrow\right|_v\hat{V}\left|\Theta\downarrow\right\rangle_c\left|-\Theta\uparrow\right\rangle_v=\left\langle\downarrow\right|_c\left\langle\uparrow\right|_v\hat{V}\left|\downarrow\right\rangle_c\left|\uparrow\right\rangle_v,\\ U'&=\left\langle\uparrow\right|_c\left\langle\uparrow\right|_v\hat{V}\left|\uparrow\right\rangle_c\left|\uparrow\right\rangle_v=\left\langle\Theta\downarrow\right|_c\left\langle-\Theta\downarrow\right|_v\hat{V}\left|\Theta\downarrow\right\rangle_c\left|-\Theta\downarrow\right\rangle_v=\left\langle\uparrow\right|_c\left\langle\uparrow\right|_v\hat{V}\left|\downarrow\right\rangle_c\left|\downarrow\right\rangle_v.\end{aligned} \tag{3-3}$$

All but two off-diagonal terms in H_{cv} are zero. For example,

$$\left\langle\uparrow\right|_c\left\langle\downarrow\right|_v H_{cv}\left|\downarrow\right\rangle_c\left|\uparrow\right\rangle_v=\left\langle\uparrow\right|_c\left\langle\downarrow\right|_v\hat{V}\left|\downarrow\right\rangle_c\left|\uparrow\right\rangle_v=I_1-I_2=0, \tag{3-4}$$

in which $\left|\uparrow\right\rangle_c\left|\downarrow\right\rangle_v=[\left|\uparrow_1\right\rangle_c\left|\downarrow_2\right\rangle_v-\left|\uparrow_2\right\rangle_c\left|\downarrow_1\right\rangle_v]/\sqrt{2}$, $\left|\downarrow\right\rangle_c\left|\uparrow\right\rangle_v=[\left|\downarrow_1\right\rangle_c\left|\uparrow_2\right\rangle_v-\left|\downarrow_2\right\rangle_c\left|\uparrow_1\right\rangle_v]/\sqrt{2}$ where we assign 1 and 2 explicitly to label two identical electrons;

$$\begin{aligned}I_1&=\left\langle\uparrow_1\right|_c\left\langle\downarrow_2\right|_v V_{12}\left|\downarrow_1\right\rangle_c\left|\uparrow_2\right\rangle_v=\left\langle\uparrow_1\right|_c\left\langle\downarrow_2\right|_v V_{12}\left|\Theta\uparrow_1\right\rangle_c\left|\uparrow_2\right\rangle_v\\ &=\left\langle\Theta^2\uparrow_1\right|_c\left\langle\downarrow_2\right|_v V_{12}\left|\Theta\uparrow_1\right\rangle_c\left|\uparrow_2\right\rangle_v=-I_1=0,\end{aligned} \tag{3-5}$$

$$\begin{aligned}I_2&=\left\langle\uparrow_1\right|_c\left\langle\downarrow_2\right|_v V_{12}\left|\downarrow_2\right\rangle_c\left|\uparrow_1\right\rangle_v=\left\langle i\Theta\uparrow_1\right|_v\left\langle\downarrow_2\right|_v V_{12}\left|i\Theta\downarrow_2\right\rangle_v\left|\uparrow_1\right\rangle_v\\ &=\left\langle\Theta\uparrow_1\right|_v\left\langle\downarrow_2\right|_v V_{12}\left|\Theta\downarrow_2\right\rangle_v\left|\Theta^2\uparrow_1\right\rangle_v=-I_2=0.\end{aligned} \tag{3-6}$$

Note that $V_{12}=V_{21}$ is the Coulomb interaction between the electron 1 and 2 and V_{12} commutes with the time-reversal operator $\Theta^2=-1$ for fermions. Other zero off-diagonal terms can be obtained by similar analysis.

Among the four two-particle states $\{\left|\uparrow\right\rangle_c\left|\downarrow\right\rangle_v,\left|\downarrow\right\rangle_c\left|\uparrow\right\rangle_v,\left|\uparrow\right\rangle_c\left|\uparrow\right\rangle_v,\left|\downarrow\right\rangle_c\left|\downarrow\right\rangle_v\}$, $\left|\uparrow\right\rangle_c\left|\uparrow\right\rangle_v$ and $\left|\downarrow\right\rangle_c\left|\downarrow\right\rangle_v$ are dark states. The optical transitions within $\left|\uparrow\right\rangle_c\left|\uparrow\right\rangle_v$ and $\left|\downarrow\right\rangle_c\left|\downarrow\right\rangle_v$ are not allowed because the spin-up (down) states are fully occupied in $\left|\uparrow\right\rangle_c\left|\uparrow\right\rangle_v$ ($\left|\downarrow\right\rangle_c\left|\downarrow\right\rangle_v$) state, while transitions between opposite spin states are forbidden.

These two dark states are irrelevant to our cascade process, and do not couple with other two bright states. Therefore, the bright exciton states must be linear combinations of two-particle bright states $|\uparrow\rangle_c|\downarrow\rangle_v$ and $|\downarrow\rangle_c|\uparrow\rangle_v$.

In the two-particle basis $\{|\uparrow\rangle_c|\downarrow\rangle_v, |\downarrow\rangle_c|\uparrow\rangle_v\}$, as we analyzed above,

$$H_{cv} = \begin{bmatrix} \epsilon_c + \epsilon_v + U & 0 \\ 0 & \epsilon_c + \epsilon_v + U \end{bmatrix}, \tag{3-7}$$

therefore $|\uparrow\rangle_c|\downarrow\rangle_v$ and $|\downarrow\rangle_c|\uparrow\rangle_v$ are degenerate bright exciton states with the same energy $\epsilon_c + \epsilon_v + U$.

The Coulomb repulsion between two electrons in the same conduction/valance level is

$$U_c = \langle\uparrow|_c \langle\downarrow|_c \hat{V} |\uparrow\rangle_c |\downarrow\rangle_c = \langle i\Theta\uparrow|_v \langle i\Theta\downarrow|_v \hat{V} |i\Theta\uparrow\rangle_v |i\Theta\downarrow\rangle_v = U_v, \tag{3-8}$$

while the Coulomb repulsion between one electron in the conduction level and another electron in the valance level is

$$U = \langle\downarrow|_c \langle\uparrow|_v \hat{V} |\downarrow\rangle_c |\uparrow\rangle_v = \langle i\Theta\downarrow|_v \langle\uparrow|_v \hat{V} |i\Theta\downarrow\rangle_v |\uparrow\rangle_v = U_v, \tag{3-9}$$

therefore $U_{c,v} = U$.

IV. Notes on Finite Element Method Simulations

To obtain the edge states in the deformed HgTe QD, we still start from the four-band effective Hamiltonian in the basis $|e,\uparrow\rangle$, $|hh,\uparrow\rangle$, $|e,\downarrow\rangle$, and $|hh,\downarrow\rangle$:

$$H_{4\times4} = \begin{bmatrix} H_\uparrow(\hat{\mathbf{k}}) & 0 \\ 0 & H_\downarrow(\hat{\mathbf{k}}) \end{bmatrix} + V(r), \tag{4-1}$$

but here $V(r)$ is the hard-wall potential with its boundary described by $r(\theta) = r_0[1 + \delta_r f(\theta)]$ in the polar coordinate system, with the mean radius $r_0 = \int_0^{2\pi} r(\theta)\,\mathrm{d}\theta/2\pi$ and the random function $f(\theta) \in [-1, 1]$ satisfies $f(\theta) = f(\theta + 2\pi)$. δ_r is a dimensionless number characterizing the maximum fluctuation percentage. Each random function for each of the QDs is generated independently as

$$f(\theta) = (1/\mathcal{N}) \sum_{n=1}^{N} c_i \sin(n\theta + \varphi_i)/\sqrt{\pi}, \tag{4-2}$$

where N is generated randomly in the interval $[10, 100]$; each $c_i(\varphi_i)$ is generated randomly and independently in the interval $[0, 2\pi]$; $\mathcal{N} = \sum_{n=1}^{N} c_i^2$. This generating scheme makes $f(\theta)$ to be a white noise. It is reasonable to model the fluctuation of a QD's boundary $f(\theta)$ as the white noise. Because the boundary of a QD formed by etching is caused by atomic dissociation process which is mesoscopically regulated and microscopically random.

When the Hamiltonian of a deformed QD is generated, we solve the Schrödinger equation for the QD with finite element method, and obtain the wavefunctions for the edge states$|\uparrow\downarrow\rangle_c$ and $|\uparrow\downarrow\rangle_v$. Then we can calculate $|c_1/c_0|^2$ as

$$\left|\frac{c_1}{c_0}\right|^2 = \left|\frac{\langle\uparrow|_v \hat{r}_+ |\uparrow\rangle_c}{\langle\uparrow|_v \hat{r}_- |\uparrow\rangle_c}\right|^2 = \left|\frac{\langle\downarrow|_v \hat{r}_- |\downarrow\rangle_c}{\langle\downarrow|_v \hat{r}_+ |\downarrow\rangle_c}\right|^2. \tag{4-3}$$